Penerbit Akademia Baru

Journal of Advanced Research in Fluid Mechanics and Thermal Sciences

Journal homepage: www.akademiabaru.com/arfmts.html
ISSN: 2289-7879

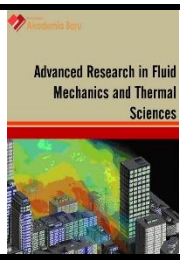

Study of Laminar Naturel Convection in Partially Porous Cavity in the Presence of Nanofluids

Open Access

Mohammed Douha[1,2,*], Belkacem Draoui[2], Noureddine Kaid[3], Houari Ameur[3], Abdellah Belkacem[2], Elmir Mohamed[2], Abdelhak Merabti[1], Houcine Aissani[1]

[1] Higher Normal School of Bechar, Bechar 08000, Algeria
[2] Laboratory of Energetic in Arid Zones (ENERGARID), University Tahri Mohamed of Bechar, P.O. Box 417, Bechar 08000, Algeria
[3] University Centre Salhi Ahmed of Naama, Institute of Science and Technology, P.O. Box 66, Naama 45000, Algeria

ARTICLE INFO

Article history:
Received 13 October 2020
Received in revised form 10 November 2020
Accepted 14 November 2020
Available online 28 December 2020

ABSTRACT

The objective of this work is the mathematical modelling and the numerical simulation of the stationary, laminar, and natural convection, in a confined square cavity ($H = L$) filled with two fluids (a mixture of nanoparticles of aluminum oxide and Al_2O_3 water) in one partition and pure water in the other partition. A porous conductive wall of thickness w ($w = L/e$) and thermal conductivity K_{eff} constitutes the exchange surface between these two partitions. The fluid movement is modeled by the Navier-Stokes equations in the two partitions, while the porous medium is modelled by the Darcy–Brinkman equation. Comsol Multiphysics software is used to solve the system of differential equations that is based on the finite element method. The results are discussed with particular attention to the mean and local Nusselt number (Nu), streamlines and isotherms. A parametric study for Rayleigh number Ra (10^2 to 10^6), volume fraction φ (0% to 10%), and Darcy number Da (10^{-7} to 10^{-2}) is performed. The obtained findings show that the increase in Ra, Da, and φ intensifies the flow and improves the thermal exchange on the cold wall. For $Da \leq 10^{-5}$, Nu remains practically low and the natural convection is being dominated by conduction. For $Da > 10^{-5}$, an increase in Nu is observed and the flows tend towards a purely convective situation. Furthermore, an increase in the heat transfer coefficients is observed with the raise of the porous layer permeability, volume fraction and Rayleigh number.

Keywords:
Laminar flow; Natural convection; Composite cavity; Porous layer; Nanofluids; Finite element method

1. Introduction

The natural convection has attracted and still attracts the interest of many researchers and engineers through its applications in several industrial sectors, such as crystal growth, solar convection, soil pollution and geology, etc. Since the discovery of the phenomenon by the

* *Corresponding author.*
E-mail address: mdouha82@gmail.com

https://doi.org/10.37934/arfmts.79.1.91110

experiments of Bénard [1] and the theoretical analysis of Rayleigh [2] at the beginning of the 20th century, the research in this field is continuous and the number of works on the subject is impressive.

To study the phenomenon of the natural convection in a porous layer, it is necessary to characterize the movement of the fluid within this layer. Due to the complexity of this porous matrix, it turns out to be impossible to know precisely the movement of the fluid saturating the porous medium. Hence, the model notion has been introduced to describe in a macroscopic way the movement of the fluid particles and the heat transfer within a porous layer.

The simplest empirical model to describe the movement of fluid within a porous layer is that of Darcy [3,4]. This model is limited to slow flows and it was later corrected to be more suitable for high Reynolds number flows. Based on experimental data, a second-order non-linear term between the infiltration rate and pressure gradients was added by Forchheimer to account for inertia effects for high-velocity flows. Wall effects (viscous stresses) are taken into account by modifying Darcy's law; the modification was presented by Brinkman [5,6].

The research by using Darcy's rule as an equation of motion were abundant in the literature. Horton and Rogers [7] and Lapwood [8] were among the first authors to conduct a natural convection study within a porous isotropic medium with uniform porosity. Since these first works, the study of convective movements within an isotropic horizontal porous layer with uniform porosity saturated by a fluid and heated from below has been the subject of a large number of works in the field of porous media [9-16]. Recently, Revnic *et al.,* [17] used a rectangular cavity of infinite dimension for the sake of putting the natural convection phenomenon with a porous medium bi-disperse based on the sample proposed by Rees *et al.,* [18]. A porous medium background composed of a solid step and pores saturated with fluid, but the solid phase can be considered as another porous medium with the same physical properties. The Rayleigh number taken in this investigation did not exceed 10^3. These authors have shown dominating conduction for great Rayleigh numbers. The dimension of the inner cell of convection contours increased with increasing Darcy number, and the thermal conductivity influenced the orientation of the central convection cell. Ismael and Chamkha [19] and Prasad [20] inspected the natural convection phenomenon in a vertical cylindrical enclosure of aspect ratio of the order of the unit filled by a porous medium generating heat, for Rayleigh numbers below 10^4. These authors found that the isothermal stratifications tighten up the sidewall of the chamber, increasing the Rayleigh number, as well as the appearance of secondary cells at higher Rayleigh numbers. The use of a Rayleigh number less than 10^4 can be explained by the fact of using Darcy's law to model the infiltration of fluid particles into the porous matrix limits the increase in *Ra*, because the law of Darcy is limited for flows at medium velocity fields. The effects of inertia and viscous stresses were not taken into account, so for large Rayleigh numbers, the problem of numerical instability arises.

Varol *et al.,* [21] studied the natural convection phenomenon in a triangular enclosure. They adopted the model of Darcy to characterize the movement of fluid within the porous matrix. The investigation has been applied for different values of Rayleigh number ($50 \leq Ra \leq 1000$) and for an aspect ratio from 0.25 to 1. They found an increase in heat transfer rates with decreasing aspect ratio. Other researchers investigated the natural convection phenomenon in a trapezoidal enclosure with constant porosity [22-24]. These investigations were made for different values of Rayleigh numbers ($100 \leq Ra \leq 1000$), inclination angle, and aspect ratio. They reported an increase in the heat transfer rate with the raise of Ra and the decrease of inclination angle. The y showed that the temperature distribution is influenced by the enclosure inclination angle, which generates a multicellular flow and influences the stratification of isotherms.

In the relation to this topic (subject), different geometries can be found in researches by Rosali *et al.,* [25], Meerikh and Mohamad [26], Phanikumar and Mahajan [27], Baytas *et al.,* [28], and

Sheremet and Pop [29]. Rosali *et al.,* [25] analyzed the unsteady boundary layer stagnation point flow and heat transfer towards a stretching sheet by considering the porosity. They found that that the skin friction coefficients decrease whereas the local Nusselt number increases with the increase in permeability parameter. Merrikh and Muhamad [26] considered in their work two vertical layers of porous media. Their concern was based on the validity of the Darcy model. As a result, they found different predictions between Darcy models and Brinkman ones. The localization of a rectangular metal form sample (of high porosity) on the bottom of a fluid-filled, heated from below was considered in the study of Phanikumar and Mahajan [27]. The investigation of Baytas *et al.,* [28] was based on the double-diffusive natural convection between a fluid and overlaying a porous medium with the stopped surface. Dramatic shifts of the heat and mass transfer were recorded in this case. Sheremet and Pop [29] used the Buongiorno's model to investigate the steady natural convection flow and heat transfer in a square porous cavity saturated by a nanofluid. Murshed *et al.,* [30] found out a significant increase in heat transfer rates with the increase of the volume concentration of the particles of nanofluid (Water/TiO_2 - water/Al_2O_3) due to the enhanced thermal conductivity and viscosity effectiveness. In addition to that, a linear increase in the thermal conductivity of nanofluids effectiveness as a function of temperature has been observed. Another interesting work on the preparation of nano-refrigerant has been reported by Halim and Sidik [31]. Kladias and Prasad [32] studied the natural convection in a horizontal porous layer heated from below. The model adopted by these authors to characterize the fluid movement in this porous layer was the Darcy model extended by Brinkman and Forchheimer (EBFD). Kangni *et al.,* [6] analysed the natural turbulence of conduction-convection in enclosures delimited by a massive wall. Varol *et al.,* [33,34] focused their study on the entropy generation due to the natural convection and conjugated heat transfer of the fluid flow within an enclosure delimited by two massive solid walls of different values of thickness.

2. Physical Model and Formulation

In this paper, we study the convection in a closed square filled with two fluids (a mixture of aluminum oxide nanoparticles Al_2O_3 and water) in one portion and pure water in the other one. A porous conductive wall of thickness w ($w = L/e$) and thermal conductivity are concerned. K_{eff} constitutes the exchange surface between the two portions mentioned previously Figure 1. Navier-Stokes equations govern the movement of the fluid in the two portions and the porous medium modelled by using the Darcy-Brinkman equation. The energy equation governs the heat transfer. Comsol Multiphysics software, which is based on the finite element method, is used to solve the differential equations system. We remind that Aluminum oxide has a chemical formula Al_2O_3. It is amphoteric in nature, and is used in various chemical, industrial and commercial applications.

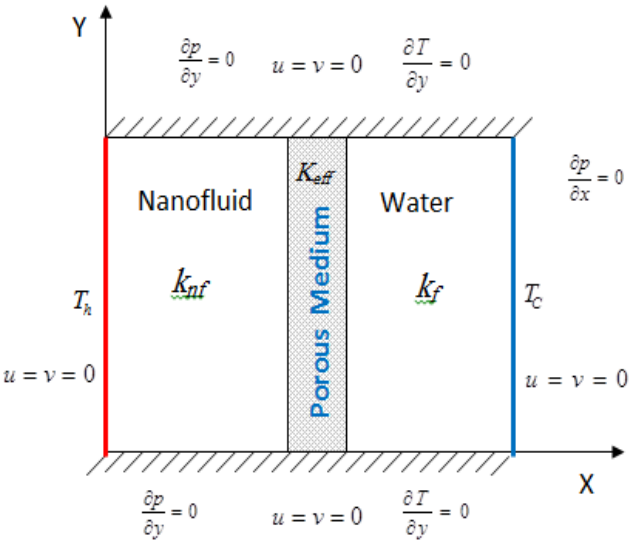

Fig. 1. Schematic of the studied configuration and boundary conditions

2.1 Hypotheses

The following assumptions are used.

i. The porous medium is saturated.
ii. The porous-fluid interface is supposed to be impermeable.
iii. The flow is two-dimensional and the fluid is incompressible.
iv. The flow regime is laminar.
v. The physical properties of the fluid and the nanofluid are both assumed to be constant.
vi. The Boussinesq [35] approximation has been taken into account.
vii. The fluid's movement in the fluid portion is led by the Navier-Stokes equations and also for the porous portion, modified by the addition of the Darcy-Brinkman term.

2.2 Mathematical Formulation

In cartesian coordinates, the governing equations of the flow of heat transfer in both the two porous and fluid portions are as follows.

The dimensional governing equations for the porous layer are as follows

Continuity

$$\frac{\partial u}{\partial x}+\frac{\partial v}{\partial y}=0 \tag{1}$$

x-Direction Momentum Equation

$$\rho_{nf}\left(u\frac{\partial u}{\partial x}+v\frac{\partial u}{\partial y}\right)=-\varepsilon^2\frac{\partial p}{\partial x}+\varepsilon\mu_{nf}\left(\frac{\partial^2 u}{\partial x^2}+\frac{\partial^2 u}{\partial y^2}\right)-\varepsilon^2\frac{\mu_{nf}}{K}u \tag{2}$$

y-Direction Momentum Equation

$$\rho_{nf}\left(u\frac{\partial v}{\partial x}+v\frac{\partial v}{\partial y}\right)=-\varepsilon^2\frac{\partial p}{\partial y}+\varepsilon\mu_{nf}\left(\frac{\partial^2 v}{\partial x^2}+\frac{\partial^2 v}{\partial y^2}\right)-\varepsilon^2\frac{\mu_{nf}}{K}v+\varepsilon^2\rho_{nf}\beta_{nf}g(T-T_0) \tag{3}$$

Energy Equation

$$u\frac{\partial T}{\partial x}+v\frac{\partial T}{\partial y}=\alpha_{eff}\left(\frac{\partial^2 T}{\partial x^2}+\frac{\partial^2 T}{\partial y^2}\right) \tag{4}$$

The dimensional equations of the nanofluid layer are as follows

Continuity

$$\frac{\partial u}{\partial x}+\frac{\partial v}{\partial y}=0 \tag{5}$$

Momentum equation in the *x*-direction

$$\rho_{nf}\left(u\frac{\partial u}{\partial x}+v\frac{\partial u}{\partial y}\right)=\frac{\partial p}{\partial x}+\mu_{nf}\left(\frac{\partial^2 u}{\partial x^2}+\frac{\partial^2 u}{\partial y^2}\right) \tag{6}$$

Momentum equation in the *y*-direction

$$\rho_{nf}\left(u\frac{\partial v}{\partial x}+v\frac{\partial v}{\partial y}\right)=-\frac{\partial p}{\partial y}+\mu_{nf}\left(\frac{\partial^2 v}{\partial x^2}+\frac{\partial^2 v}{\partial y^2}\right)+\rho_{nf}\beta_{nf}g(T-T_0) \tag{7}$$

Energy Equation

$$u\frac{\partial T}{\partial x}+v\frac{\partial T}{\partial y}=\alpha_{nf}\left(\frac{\partial^2 T}{\partial x^2}+\frac{\partial^2 T}{\partial y^2}\right) \tag{8}$$

The adopted relations that prescribe the physical properties of the nanofluid in Table 1 are as follows.

Table 1
Physical property of nanoparticles and water at T = 20 °C

	Pr	ρ (kg/m^3)	C_p (J/kg.K)	*K* (W/m.K)	*B* ($\times 10^{-5}$) (K^{-1})
Water	6.2	998.2	4181.8	0.593	21
Al_2O_3		3960.14	761.55	37.17	0.75

The significant density of a fluid containing suspended particles at a reference temperature is given by

$$\rho_{nf}=(1-\phi)\rho_f+\phi\rho_s \tag{9}$$

$$(\rho\beta)_{nf}=(1-\phi)(\rho\beta)_f+\phi(\rho\beta)_s \tag{10}$$

The heat capacity of the nanofluid can be written as

$$(\rho C_P)_{nf}=(1-\phi)(\rho C_P)_f+\phi(\rho C_P)_s \tag{11}$$

where φ, ρ_f, and ρ_s are the volume fraction of the suspended particles, density of the particles and based fluid, respectively. The viscosity effectiveness of nanofluid that consists of pure water and a dilute suspension of tiny solid spherical particles is given by Brinkman as shown below

$$\mu_{nf} = \frac{\mu_f}{(1-\phi)^{2.5}} \tag{12}$$

The stagnant thermal conductivity of the solid-liquid mixture was first developed by Wasp

$$k_{nf} = k_f(-13\phi^2 + 6.3\phi + 1) \tag{13}$$

The thermal diffusivity of nanofluid α_{nf} is evaluated from

$$\alpha_{nf} = \frac{k_{nf}}{(\rho C_p)_{nf}} \tag{14}$$

The following dimensionless variables are defined

$$X = \frac{x}{L} \; ; \; Y = \frac{y}{L} \; ; \; U = \frac{uL}{\alpha_f} \; ; \; V = \frac{vuL}{\alpha_f} \; ; \; P = \frac{pL^2}{\rho_{nf}\alpha_f^2} \; ; \; \theta = \frac{T-T_f}{\Delta T} \; avec \; \Delta T = T_c - T_f \tag{15}$$

As a result, the non-dimensional equation of conservation can be written as the same way for the porous layer

Continuity

$$\frac{\partial U}{\partial X} + \frac{\partial V}{\partial Y} = 0 \tag{16}$$

Momentum equation in the *x*-direction

$$U\frac{\partial U}{\partial X} + V\frac{\partial U}{\partial Y} = -\frac{\partial P}{\partial X} + \varepsilon\frac{Pr}{(1-\phi)^{2.5}(1-\phi+R_\rho\phi)} \times \left(\frac{\partial^2 U}{\partial X^2} + \frac{\partial^2 U}{\partial Y^2}\right) - \varepsilon^2\frac{Pr}{Da\frac{1}{(1-\phi)^{2.5}(1-\phi+R_\rho\phi)}} \tag{17}$$

Momentum equation in the *y*-direction

$$U\frac{\partial V}{\partial X} + V\frac{\partial V}{\partial Y} = -\frac{\partial P}{\partial Y} + \varepsilon\frac{Pr}{(1-\phi)^{2.5}(1-\phi+R_\rho\phi)} \times \left(\frac{\partial^2 V}{\partial X^2} + \frac{\partial^2 V}{\partial Y^2}\right) - \varepsilon^2\frac{Pr}{Da\frac{1}{(1-\phi)^{2.5}(1-\phi+R_\rho\phi)}} + \varepsilon^2\frac{(1-\phi+R_\rho R_\beta\phi)}{(1-\phi+R_\rho\phi)} Ra\, Pr\, \theta \tag{18}$$

Energy Equation

$$U\frac{\partial \theta}{\partial X} + v\frac{\partial \theta}{\partial Y} = \frac{\alpha_{eff}}{\alpha_f}\left(\frac{\partial^2 \theta}{\partial X^2} + \frac{\partial^2 \theta}{\partial Y^2}\right) \tag{19}$$

For nanofluid (nonporous layer)

Continuity

$$\frac{\partial U}{\partial X} + \frac{\partial V}{\partial Y} = 0 \tag{20}$$

Momentum equation in the *x*-direction

$$U\frac{\partial U}{\partial X}+V\frac{\partial U}{\partial Y}=-\frac{\partial P}{\partial X}+\frac{Pr}{(1-\phi)^{2.5}(1-\phi+R_\rho\phi)}\times\left(\frac{\partial^2 U}{\partial X^2}+\frac{\partial^2 U}{\partial V^2}\right) \tag{21}$$

Momentum equation in the *y*-direction

$$U\frac{\partial V}{\partial X}+V\frac{\partial V}{\partial Y}=\frac{\partial P}{\partial Y}+\frac{Pr}{(1-\phi)^{2.5}(1-\phi+R_\rho\phi)}\times\left(\frac{\partial^2 V}{\partial X^2}+\frac{\partial^2 V}{\partial Y^2}\right)+\frac{(1-\phi+R_\rho R_\beta\phi)}{(1-\phi+R_\rho\phi)}Ra\,Pr\,\theta \tag{22}$$

Energy Equation

$$U\frac{\partial \theta}{\partial X}+v\frac{\partial \theta}{\partial Y}=\frac{\alpha_{nf}}{\alpha_f}\left(\frac{\partial^2 \theta}{\partial X^2}+\frac{\partial^2 \theta}{\partial Y^2}\right) \tag{23}$$

where the following dimensionless numbers appear.

$$Ra=\frac{g\beta_f\Delta TL^3}{\alpha_f\nu_f};Da=\frac{K}{L^2};Pr\ =\ \frac{\nu}{\alpha_f}$$
$$R_\rho=\frac{\rho_s}{\rho_f};R_\beta=\frac{\beta_s}{\beta_f}; \tag{24}$$

The local and average Nusselt numbers along the right wall are calculated, respectively, as below.

$$Nu_{local}=\frac{k_{nf}}{k_f}\frac{\partial \theta_{nf}}{\partial X}\bigg|_{X=L} \tag{25}$$

$$Nu_{avg}=\frac{k_{nf}}{k_f}\int_0^L\frac{\partial \theta_{nf}}{\partial X}\bigg|_{X=L}dY \tag{26}$$

3. Numerical Computations

The numerical method to solve the governing equations of the physical problem remain an efficient and less expensive technique for the treatment of various industrial applications [38-40]. In this paper, the study has been achieved numerically by using the computer software COMSOL. It is a powerful and interactive tool for modelling various scientific problems of fluid flows and heat transfer. It is based on the finite element method to solve the governing equations of the problem. It is as a stand-alone product and it is accessed through a flexible graphical user interface, or script programming in the MATLAB language.

The numerical results are obtained by solving the system of Eq. (1)-(8), with the appropriate boundary conditions. The two-dimensional spatial domain is divided into quadratic elements (mesh structured) as shown in Figure 2. The mesh is refined near the borders. A nonlinear solver was used, and the convergence criterion was fixed to 10^6.

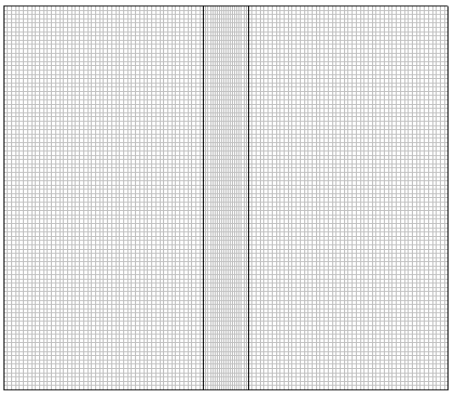

Fig. 2. Schematic of the mesh used

4. Results and Discussion

The reliability of the computer software and the numerical method adopted was checked by validating our predictions against some experimental data of the literature. For this purpose, we referred to the works of Khanafer *et al.,* [36] and Lauriat and Prasad [37]. It concerns differentially heated cavities, fully porous and filled with Al_2O_3 nanofluid. The results of comparison are shown in Table 2, where a good agreement is observed.

Table 2
Comparisons of the present numerical solutions with previous works

	Ra	*Da*	Lauriat and Prasad [37]	Present work
Porous	10^3	10^{-2}	1.02	1.0001
Cavity	10^5	10^{-2}	3.8	3.65
$\varepsilon = 0.4$	10^7	10^{-6}	1.08	1.11
$Pr = 1$	10^8	10^{-6}	2.99	3.02
	Ra	φ	Khanafer *et al.,* [36]	Present work
Nano-fluid	10^3	0.04	2.08	2.11
Cavity	10^5	0.08	2.24	2.20
$Pr = 6.2$	10^5	0.04	8.93	8.67
	10^5	0.08	9.6	9.34

To describe the effect of the porous zone on the structure of the flow in the partitioning cavity, the following control parameters are set: $Pr = 6.2$, $\varepsilon = 0.4$, $R_\rho = 3.79$, $R_\beta = 0.036$.

Figure 6 to Figure 10 present the current function and isotherms for a uniform porosity $\varepsilon = 0.4$ and different Rayleigh numbers *Ra* (10^4, 10^5, and 10^6), Darcy numbers *Da* (10^{-7}, 10^{-5}, 10^{-3}, and 10^{-2}), and volume fractions φ (0%, 4%, and 8%). These figures are plotted to illustrate the effect of these variables on the flow and heat transfer. The convection begins with a single-cell flow in the two partitions of very variable intensity (Table 3) and with the absence of cells in the porous zone. The cell of the porous zone exhibits a vortex that widens with increasing volume fraction. For $Da = 10^{-7}$, unequal vortices of the two partitions are observed. The isotherms are almost parallel, that is to say that the heat transfer is purely conductive for $Ra = 10^4$, Da = (10^{-7} and 10^{-5}), and φ = (0%, 4%, and 8%). The isotherms start to deform by increasing Raleigh numbers, thus altering the convection birth in the fluid zone.

The isotherms sink towards the fluid zone and change the predominating convection over the conduction. The isotherms are parallel in the porous zone beside the vertical wall. As a fact, the thermal flow takes on a conductive aspect so there is a slight deformation of the isotherms in this zone. For $Ra = 10^6$, $Da = 10^{-5}$, and $\varphi = 8\%$, the steady-state is reached and the isotherms take place in

the entire volume of the cavity. The heated air particles rise next to the interface, then the cooled particles flow along the right wall. The convective mode is dominant in this situation.

For $Ra = 10^4$ and $\varphi = 0\%$, the flow is intensified by increasing Da (10^{-2}, 10^{-3}), while it remains a single-cell with a rectangular structure filling the two partitions and rotating in the anti-trigonometric direction as shown in Figure 7.

For $\varphi = 4$ and 8%, the flow intensification is clearly seen, also an increase in the Darcy number can be noticed in an impermeability increase, which gives much more freedom for fluid convection.

The transfer regime is conductive for $Ra = 10^4$, $\varphi = 0\%$, and Da = (10^{-2}, 10^{-3}), where the shape of the isotherms begins to deform as shown in Figure 3 and 4, and the birth of convection is observed. For $Ra = 10^5$ and 10^6, the isotherms take place throughout the volume of the cavity in the form 'S' as shown in Figure 5 and 6 while a convective flow appears in the ascending direction near the interface of the cold wall as shown in Figure 6. For $\varphi = 4$ and 8%, the convection increases and overcomes the conduction.

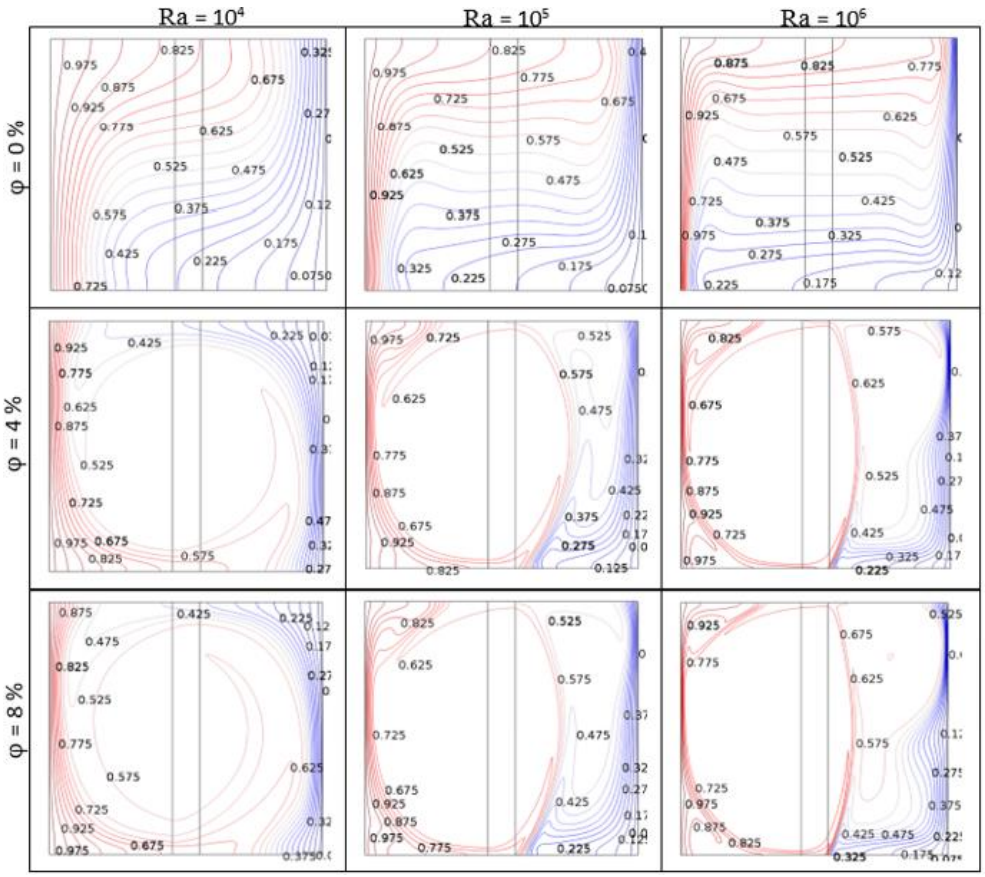

Fig. 3. Thermal distribution for $Da = 10^{-2}$

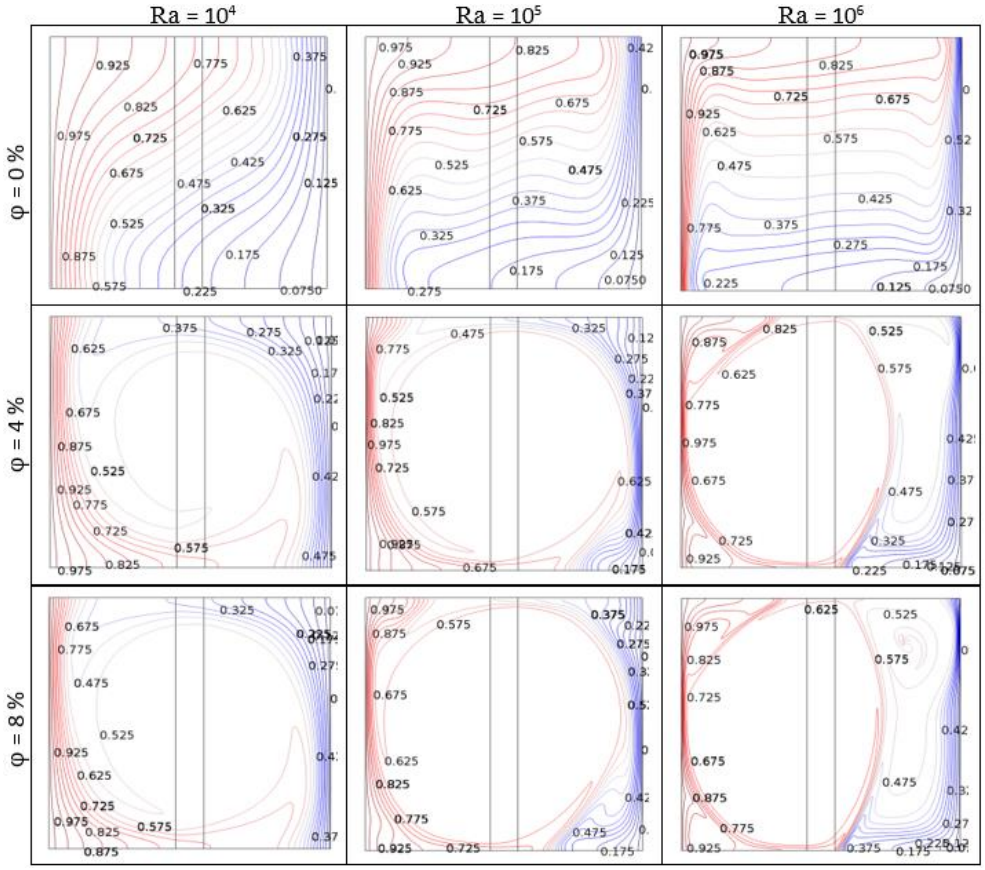

Fig. 4. Thermal distribution for $Da = 10^{-3}$

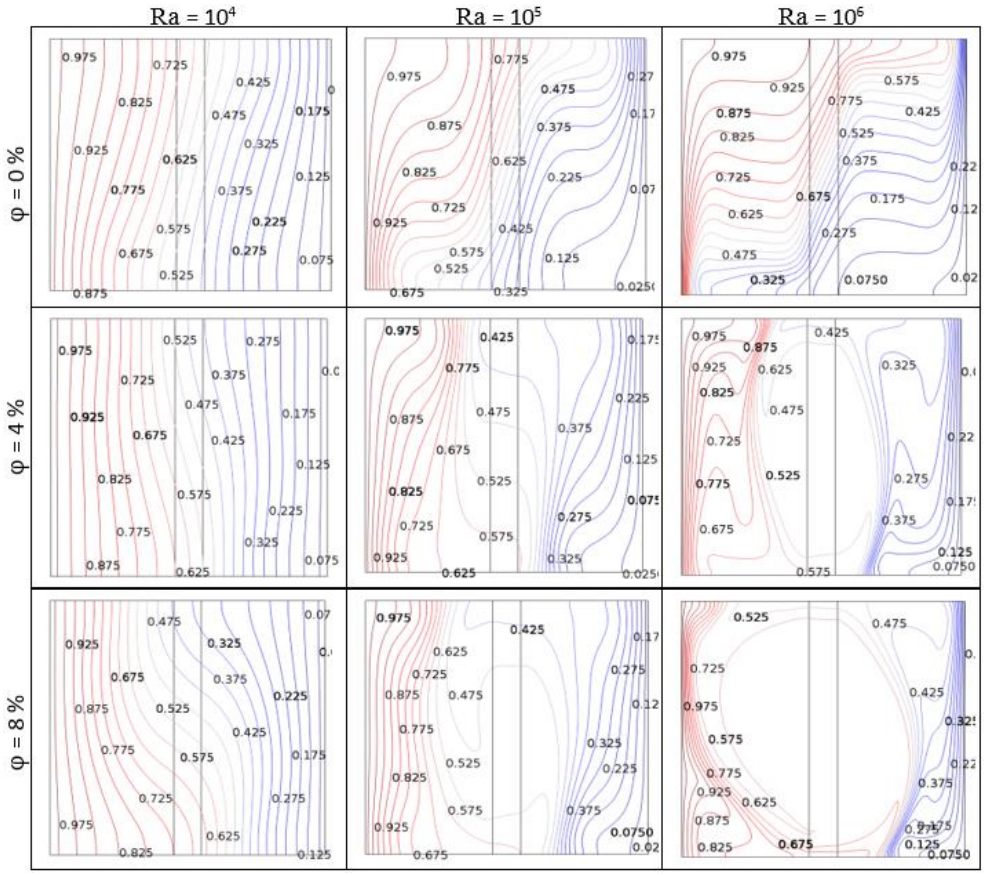

Fig. 5. Thermal distribution for $Da = 10^{-5}$

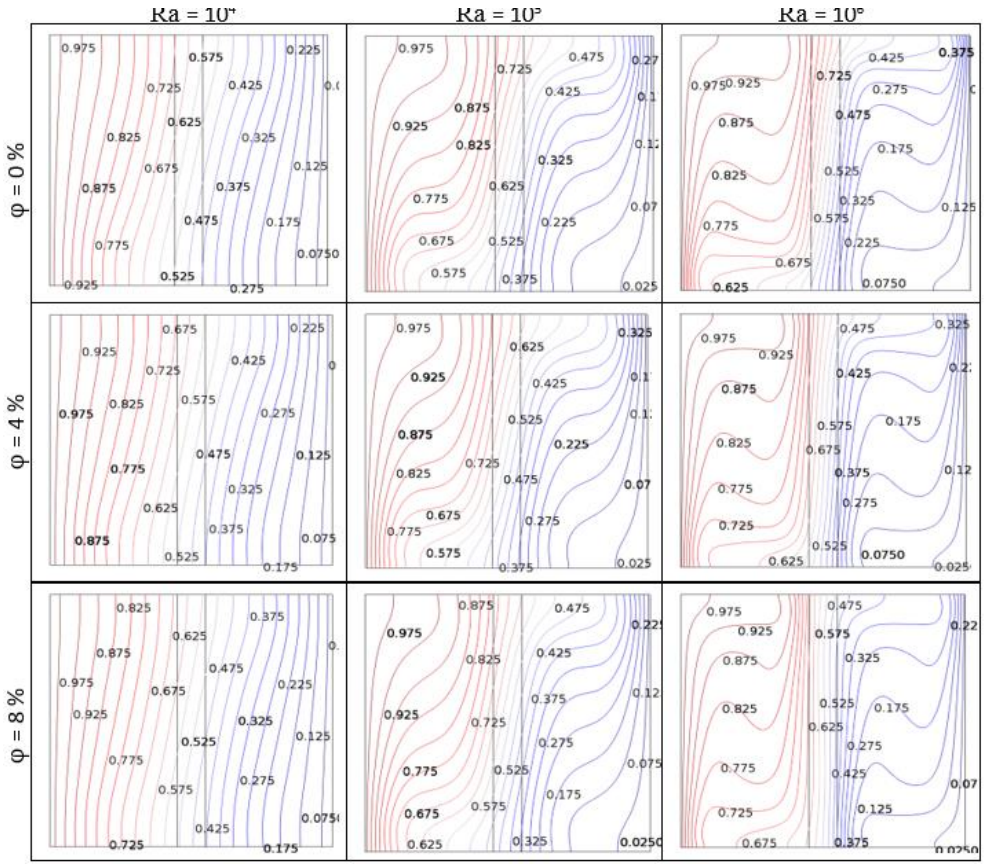

Fig. 6. Thermal distribution for $Da = 10^{-7}$

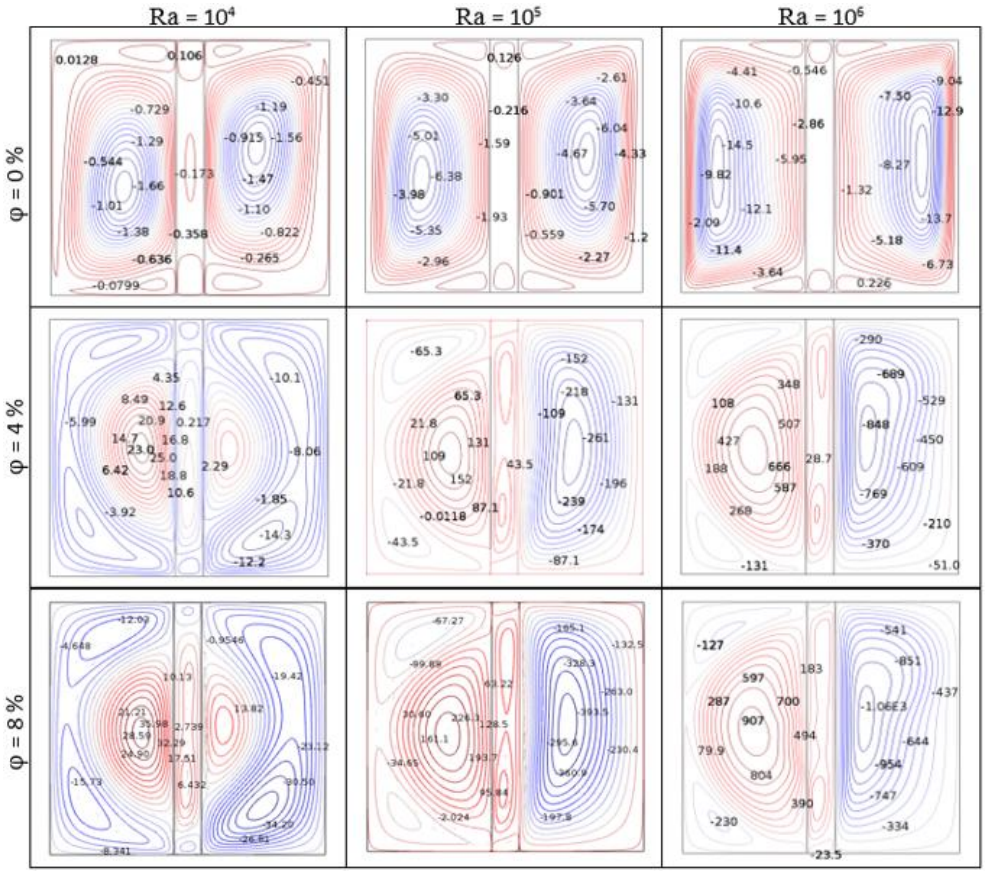

Fig. 7. Distribution of the current lines for $Da = 10^{-2}$

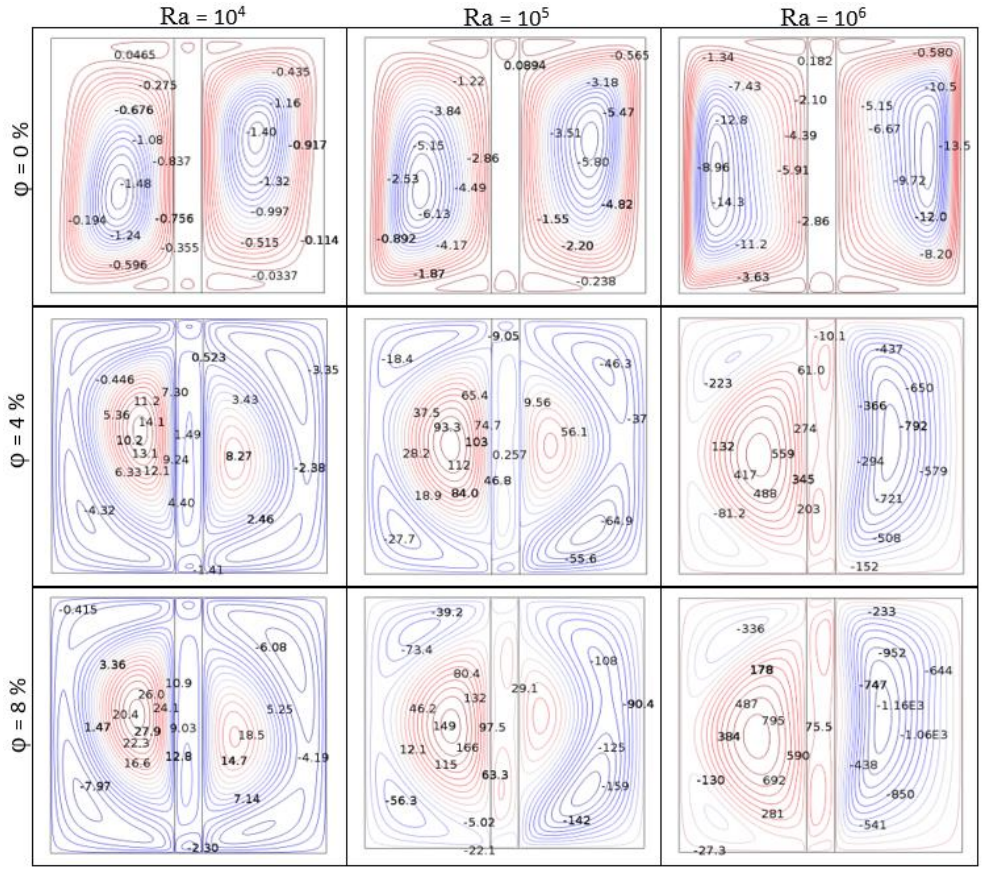

Fig. 8. Distribution of the current lines for $Da = 10^{-3}$

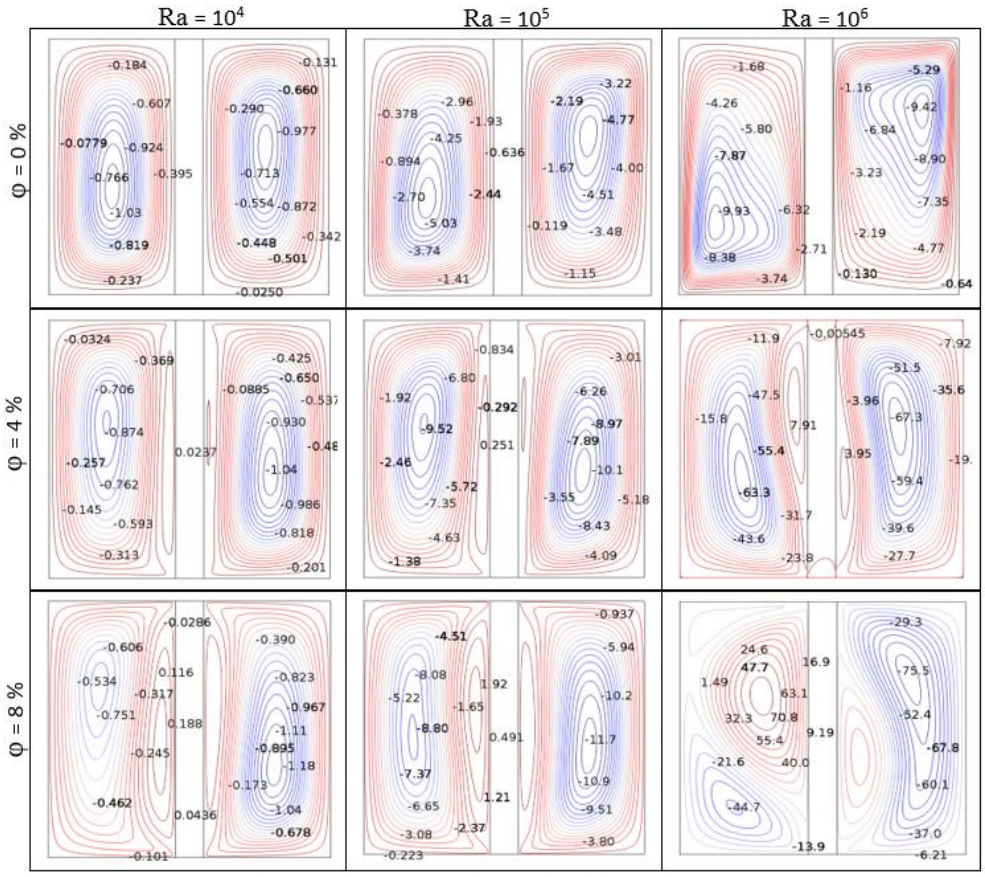

Fig. 9. Distribution of the current lines for $Da = 10^{-5}$

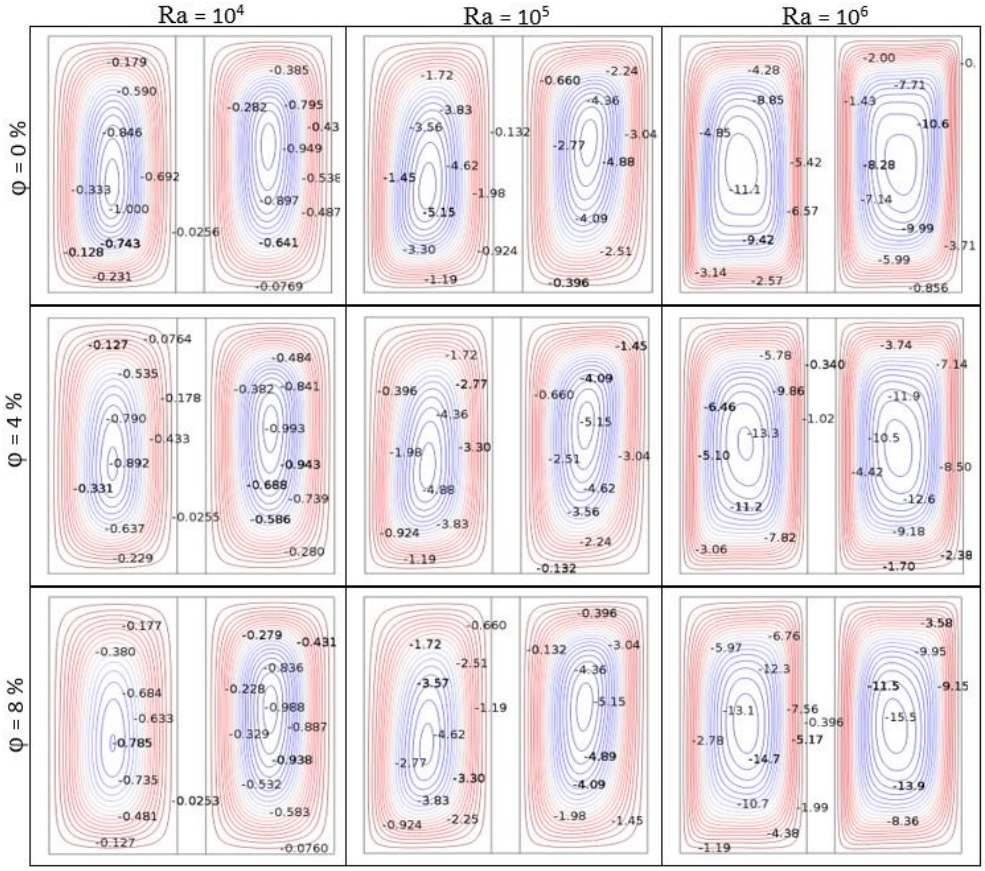

Fig. 10. Distribution of the current lines for *Da* = 10^{-7}

Table 3
The minimal and maximal values of the current function for different *Ra*, φ, and *Da*

	Da =10^{-2}						Da =10^{-5}					
	Ra = 10^4		Ra = 10^4		Ra = 10^5		Ra = 10^4		Ra = 10^5		Ra = 10^6	
	$\lvert\Psi\rvert_{min}$	$\lvert\Psi\rvert_{min}$	$\lvert\Psi\rvert_{max}$	$\lvert\Psi\rvert_{min}$	$\lvert\Psi\rvert_{min}$	$\lvert\Psi\rvert_{max}$	$\lvert\Psi\rvert_{min}$	$\lvert\Psi\rvert_{max}$	$\lvert\Psi\rvert_{min}$	$\lvert\Psi\rvert_{min}$	$\lvert\Psi\rvert_{max}$	$\lvert\Psi\rvert_{min}$
φ = 0 %	0,1056	0,025	1,0303	0,1192	5,0285	0,1303	0,025	1,0303	0,1192	5,0285	0,1303	9,9316
φ = 4 %	14,265	0,0237	1,0422	0,2509	10,06	7,9121	0,0237	1,0422	0,2509	10,06	7,9121	67,305
φ = 8 %	34,196	0,188	1,1837	1,9201	11,654	70,763	0,188	1,1837	1,9201	11,654	70,763	75,484
	Da = 10^{-3}						Da =10^{-7}					
	Ra = 10^4		Ra = 10^4		Ra = 10^5		Ra = 10^4		Ra = 10^5		Ra = 10^6	
	$\lvert\Psi\rvert_{min}$	$\lvert\Psi\rvert_{min}$	$\lvert\Psi\rvert_{max}$	$\lvert\Psi\rvert_{min}$	$\lvert\Psi\rvert_{min}$	$\lvert\Psi\rvert_{max}$	$\lvert\Psi\rvert_{min}$	$\lvert\Psi\rvert_{max}$	$\lvert\Psi\rvert_{min}$	$\lvert\Psi\rvert_{min}$	$\lvert\Psi\rvert_{max}$	$\lvert\Psi\rvert_{min}$
φ = 0 %	0,0465	0,0256	0,9998	0,1319	5,1477	0,2853	0,0256	0,9998	0,1319	5,1477	0,2853	11,133
φ = 4 %	4,3183	0,0255	0,9935	0,132	5,1488	0,3399	0,0255	0,9935	0,132	5,1488	0,3399	13,263
φ = 8 %	7,9735	0,0253	0,9882	0,132	5,1508	0,3965	0,0253	0,9882	0,132	5,1508	0,3965	15,52

Figure 11 shows the promotion of heat transfer for a wide range of *Da* varying from 10^{-6} to 10^{-2}. For *Ra* = (10^2 to 10^6) and φ = (0, 4, and 8%), an increase in *Nu* is observed with *Da* as shown in Figure 12.

That is because the increase in permeability leads to an increase in Darcy number, resulting thus in an intensification of the movement of the fluid particles and enhanced heat transfer.

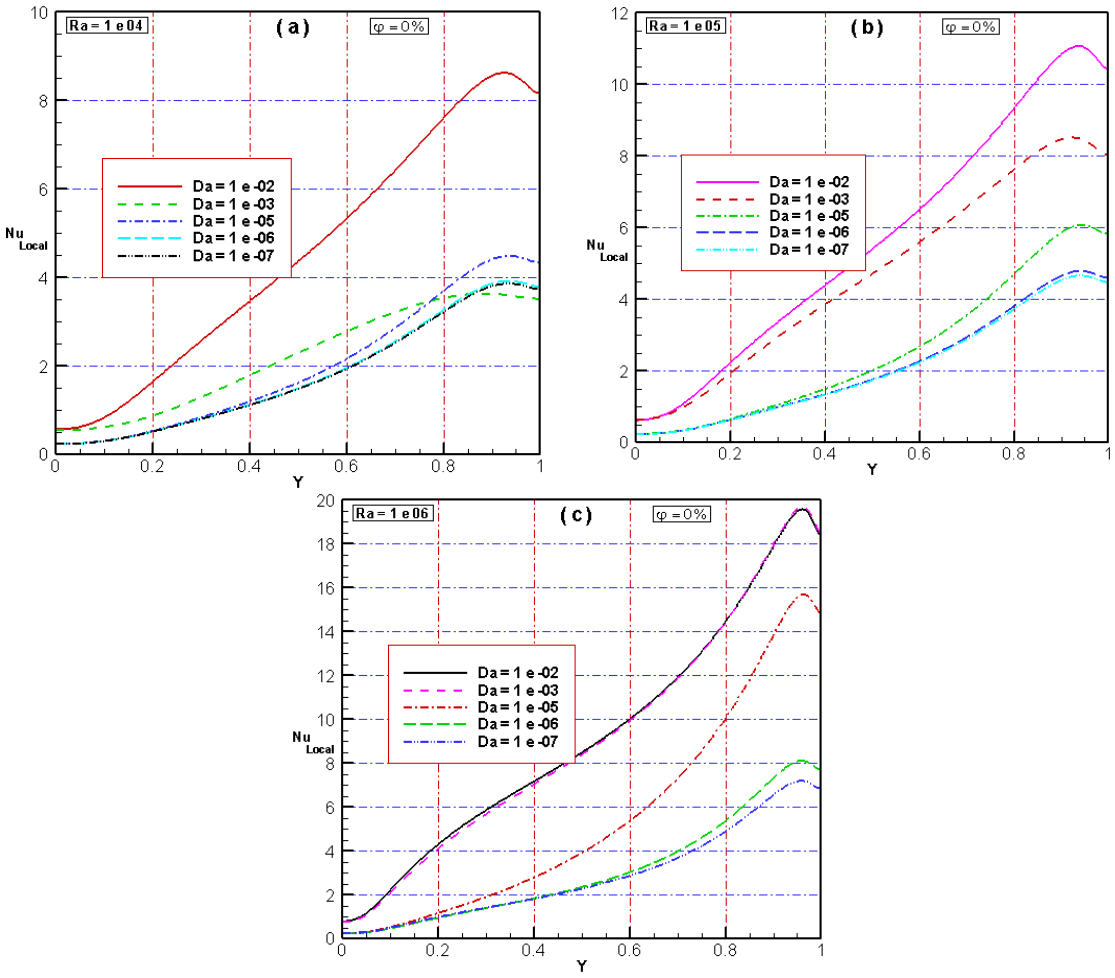

Fig. 11. Variation of the local Nusselt number along the wall$_2$ for $\varphi = 0$ %, (a) $Ra = 10^4$; (b) $Ra = 10^5$; (c) $Ra = 10^6$

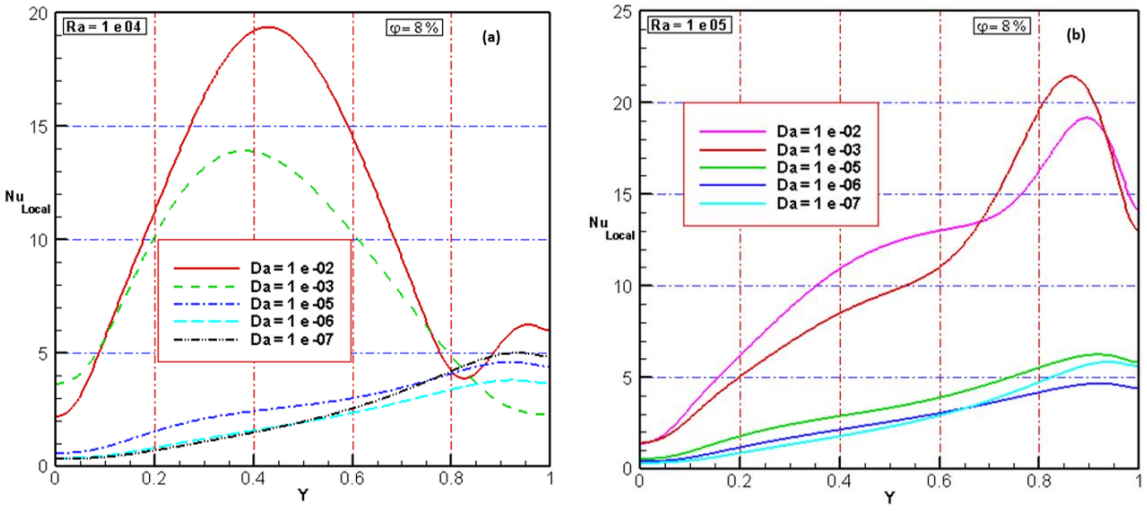

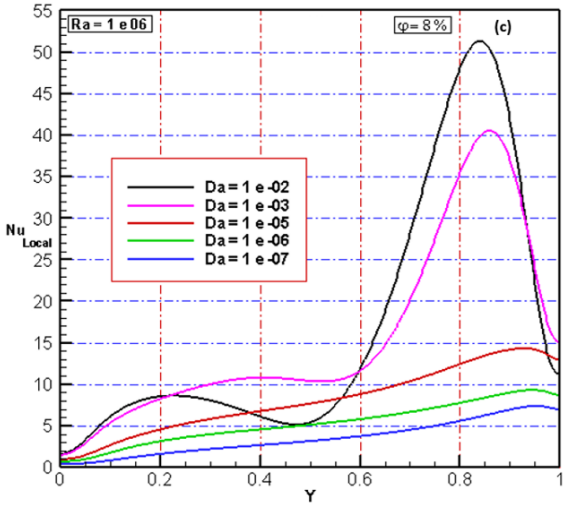

Fig. 12. Variation of the local Nusselt number along the wall$_2$ for φ = 8 %, (a) *Ra* = 10^4; (b) *Ra* = 10^5; (c) *Ra* = 10^6

For a fixed Darcy number (*Da* = 10^{-2}), the effects of Rayleigh number (*Ra* = 10^4, 10^5, and 10^6), as well as the nanofluid volume fraction (φ = 0, 2, 4, 6, and 8%) are examined and highlighted in Figure 13(a)-(c). On another hand, the figures reveal the addition of the nanoparticles noticeably improves heat transfer, particularly for high values of the Rayleigh number.

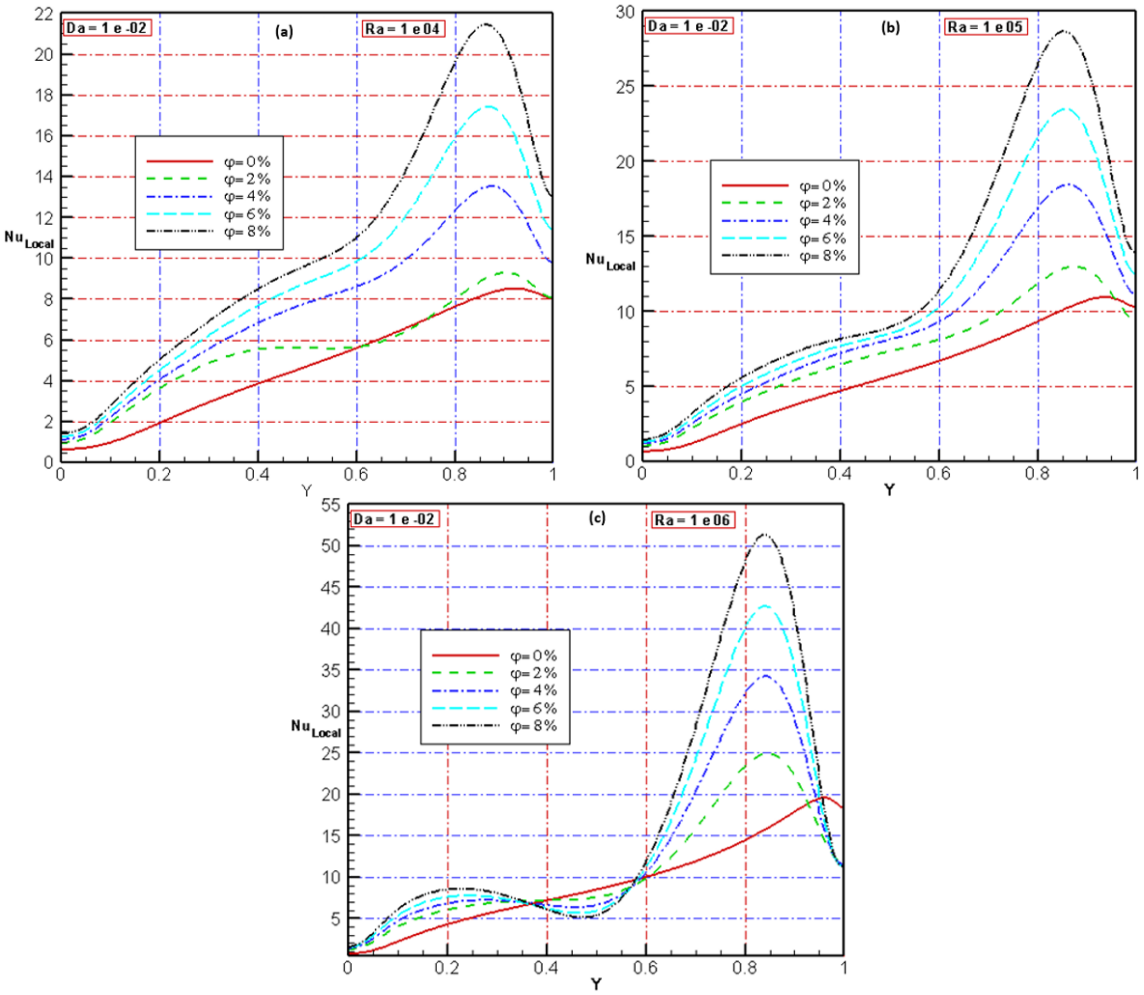

Fig. 13. Variation of the local Nusselt number along the wall$_2$ for *Da* = 10^{-2}, (a) *Ra* = 10^4; (b) *Ra* = 10^5; (c) *Ra* = 10^6

Figure 14(a)-(c) show that for $Da = 10^{-7}$ the fraction volume has a negligible effect on the local Nusselt number. Even for $Ra = 10^6$, the Darcy range behaves like an impermeable area for the porous medium is concerned, where the flow is nearly negligible. This means that the thermal exchange is mainly achieved by conduction.

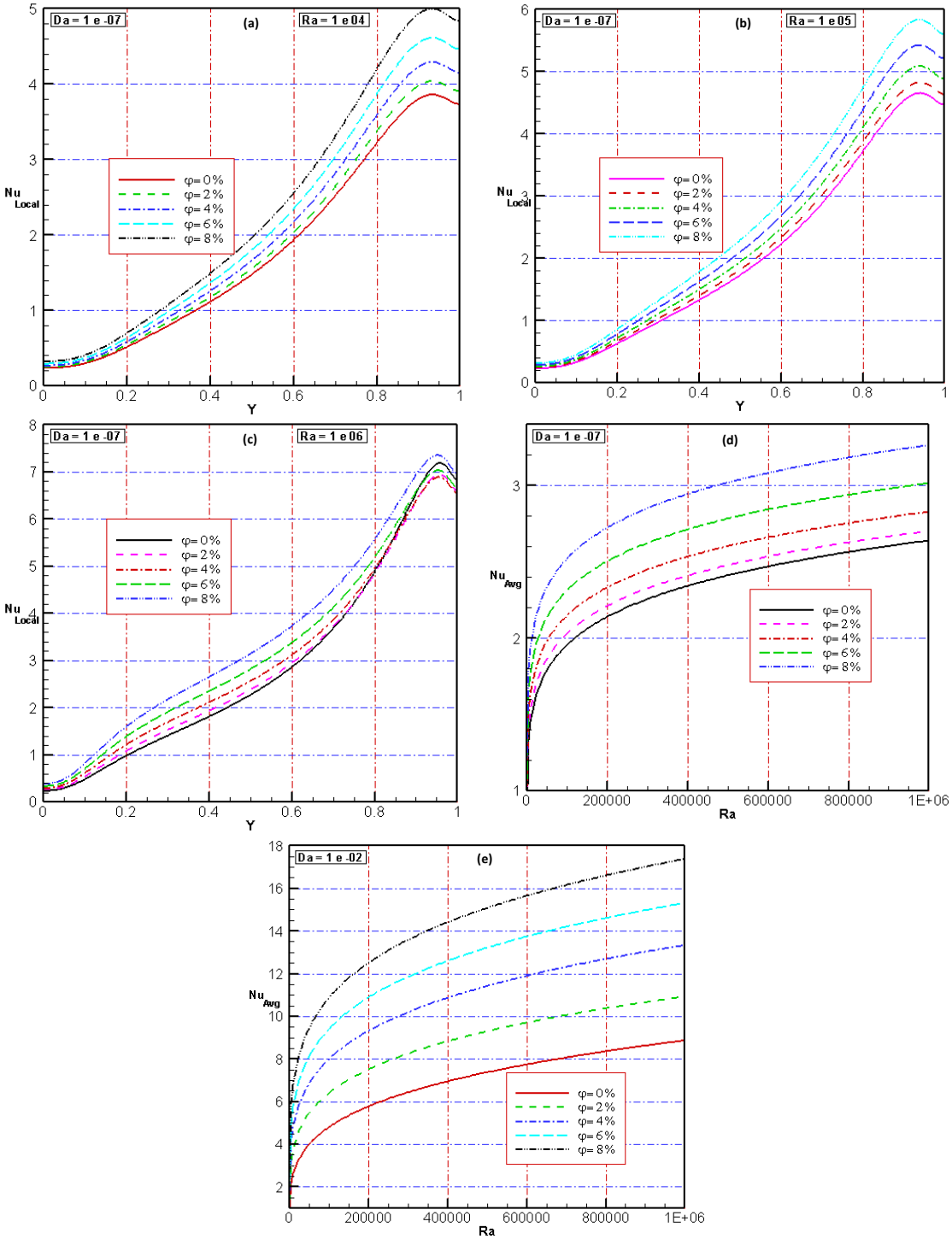

Fig. 14. Variation of the average Nusselt number along the wall$_2$, (a) (for $Da = 10^{-7}$) Ra = 10^4; (b) (for $Da = 10^{-7}$) Ra = 10^5; (c) (for $Da = 10^{-7}$) Ra = 10^6; (d) $Da = 10^{-7}$; (e) $Da = 10^{-2}$

For *Da* = (10^{-7}, 10^{-2}), Figure 14(d) and Figure 14(e) illustrate the effect of the volume fraction on the average Nusselt number *vs. Ra*. The results indicate a notable improvement in the heat transfer within the cavity for φ = 8% as shown in Figure 12 and Figure 15(b). This improvement is more significant in the case of *Da* = 10^{-2}. These results agree well with the literature [41-43].

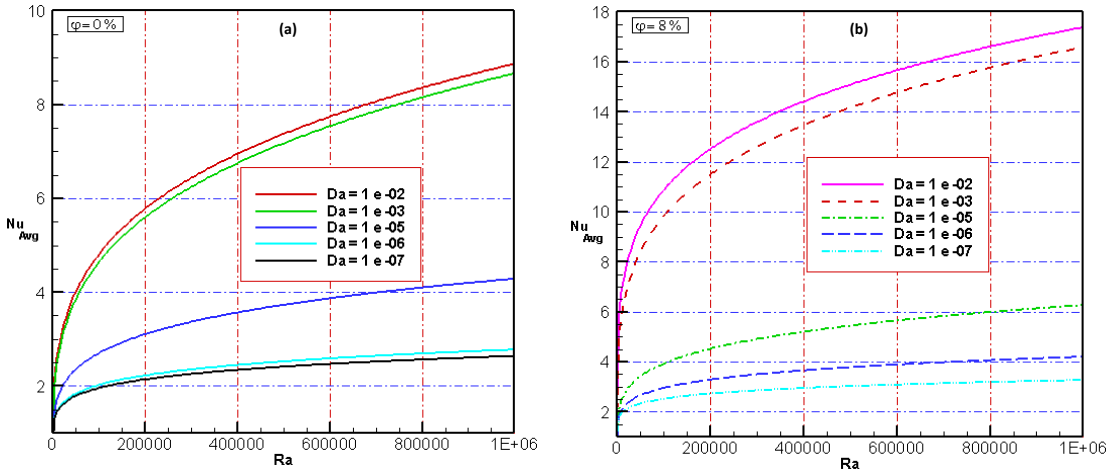

Fig. 15. Variation of the average Nusselt number along the wall$_2$ (a) φ = 0%; (b) φ = 8%

5. Conclusion

The natural convection within a confined square cavity *H* = *L* has been numerically investigated. The cavity was divided into two partitions filled of two fluids (a mixture of nanoparticles of aluminium oxide Al_2O_3 and water). A porous conductive wall (ε = 0.4) of thickness *w* (*w* = *L*/*e*) and of thermal conductivity K_{eff} constitutes the surface exchange between the two partitions. The effects of Darcy number effects (*Da*), volume fraction (φ), and the Rayleigh number (*Ra*) were analysed.

The obtained results revealed that the increase in *Ra*, *Da*, and φ intensifies the flow Table 3 and improves the heat transfer on the cold wall. The values of Nusselt numbers remained practically low due to the low considered values of permeability ($Da \leq 10^{-5}$) as shown in Figure 15. Aa a consequence, the porous medium in this Darcy range behaves the same way as an impermeable zone where the flow is nearly negligible, and the natural convection is being dominated by conduction.

For $Da > 10^{-5}$, an increase in Nusselt number was observed and the flows tend towards a purely convective situation.

The influence of the porous layer permeability on the transfer rates has been also analysed. An increase in the heat transfer coefficients was observed with the raise of the porous layer permeability, volume fraction and Rayleigh number.

References

[1] Bénard, Henri. "Les Tourbillons cellulaires dans une nappe liquide transportant de la chaleur par convection en regime permanent." In *Annales de Chimie et de Physique*, vol. 23, pp. 62-144. 1901.

[2] Rayleigh, Lord. "LIX. On convection currents in a horizontal layer of fluid, when the higher temperature is on the under side." *The London, Edinburgh, and Dublin Philosophical Magazine and Journal of Science* 32, no. 192 (1916): 529-546. https://doi.org/10.1080/14786441608635602

[3] Stern, Melvin E. "Collective instability of salt fingers." *Journal of Fluid Mechanics* 35, no. 2 (1969): 209-218. https://doi.org/10.1017/S0022112069001066

[4] Bejan, Adrian. "On the boundary layer regime in a vertical enclosure filled with a porous medium." *Letters in Heat and Mass Transfer* 6, no. 2 (1979): 93-102. https://doi.org/10.1016/0094-4548(79)90001-8

[5] Lee, T. S. "Numerical experiments with fluid convection in tilted nonrectangular enclosures." *Numerical Heat Transfer* 19, no. 4 (1991): 487-499. https://doi.org/10.1080/10407789108944861
[6] Kangni, A., R. Ben Yedder, and E. Bilgen. "Natural convection and conduction in enclosures with multiple vertical partitions." *International Journal of Heat and Mass Transfer* 34, no. 11 (1991): 2819-2825. https://doi.org/10.1016/0017-9310(91)90242-7
[7] Horton, C. W., and F. T. Rogers Jr. "Convection currents in a porous medium." *Journal of Applied Physics* 16, no. 6 (1945): 367-370. https://doi.org/10.1063/1.1707601
[8] Lapwood, ER303660032. "Convection of a fluid in a porous medium." In *Mathematical Proceedings of the Cambridge Philosophical Society*, vol. 44, no. 4, pp. 508-521. Cambridge University Press, 1948. https://doi.org/10.1017/S030500410002452X
[9] Manole, D. M., and J. L. Lage. "Numerical benchmark results for natural convection in a porous medium cavity." In *Heat and Mass Transfer in Porous Media, ASME Conference 1992*, vol. 216, pp. 55-60. 1992.
[10] Baytas, A. Cihat, and Ioan Pop. "Free convection in a square porous cavity using a thermal nonequilibrium model." *International Journal of Thermal Sciences* 41, no. 9 (2002): 861-870. https://doi.org/10.1016/S1290-0729(02)01379-0
[11] Kumar, BV Rathish, P. Singh, and V. J. Bansod. "Effect of thermal stratification on double-diffusive natural convection in a vertical porous enclosure." *Numerical Heat Transfer: Part A: Applications* 41, no. 4 (2002): 421-447. https://doi.org/10.1080/104077802317261254
[12] Bourich, M., M. Hasnaoui, and A. Amahmid. "Double-diffusive natural convection in a porous enclosure partially heated from below and differentially salted." *International Journal of Heat and Fluid Flow* 25, no. 6 (2004): 1034-1046. https://doi.org/10.1016/j.ijheatfluidflow.2004.01.003
[13] Kim, Gi Bin, and Jae Min Hyun. "Buoyant convection of a power-law fluid in an enclosure filled with heat-generating porous media." *Numerical Heat Transfer, Part A: Applications* 45, no. 6 (2004): 569-582. https://doi.org/10.1080/10407780490277572
[14] Oztop, Hakan F. "Combined convection heat transfer in a porous lid-driven enclosure due to heater with finite length." *International Communications in Heat and Mass Transfer* 33, no. 6 (2006): 772-779. https://doi.org/10.1016/j.icheatmasstransfer.2006.02.003
[15] Pakdee, W., and P. Rattanadecho. "Unsteady effects on natural convective heat transfer through porous media in cavity due to top surface partial convection." *Applied Thermal Engineering* 26, no. 17-18 (2006): 2316-2326. https://doi.org/10.1016/j.applthermaleng.2006.03.004
[16] Ould-Amer, Yacine, and Saoussène Slama. "Convection naturelle dans un milieu poreux multicouche." *JITH, Albi, France* (2007).
[17] Revnic, C., T. Grosan, I. Pop, and D. B. Ingham. "Free convection in a square cavity filled with a bidisperse porous medium." *International Journal of Thermal Sciences* 48, no. 10 (2009): 1876-1883. https://doi.org/10.1016/j.ijthermalsci.2009.02.016
[18] Rees, D. A. S., D. A. Nield, and A. V. Kuznetsov. "Vertical free convective boundary-layer flow in a bidisperse porous medium." *Journal of Heat Transfer* 130, no. 9 (2008): 1-9. https://doi.org/10.1115/1.2943304
[19] Ismael, Muneer A., and Ali J. Chamkha. "Conjugate natural convection in a differentially heated composite enclosure filled with a nanofluid." *Journal of Porous Media* 18, no. 7 (2015): 699-716. https://doi.org/10.1615/JPorMedia.v18.i7.50
[20] Prasad, V. "Numerical study of natural convection in a vertical, porous annulus with constant heat flux on the inner wall." *International Journal of Heat and Mass Transfer* 29, no. 6 (1986): 841-853. https://doi.org/10.1016/0017-9310(86)90180-8
[21] Varol, Yasin, Hakan F. Oztop, and Asaf Varol. "Free convection in porous media filled right-angle triangular enclosures." *International Communications in Heat and Mass Transfer* 33, no. 10 (2006): 1190-1197. https://doi.org/10.1016/j.icheatmasstransfer.2006.08.008
[22] Baytaş, A. C., and I. Pop. "Natural convection in a trapezoidal enclosure filled with a porous medium." *International Journal of Engineering Science* 39, no. 2 (2001): 125-134. https://doi.org/10.1016/S0020-7225(00)00033-1
[23] Kumar, BV Rathish, and Bipin Kumar. "Parallel computation of natural convection in trapezoidal porous enclosures." *Mathematics and Computers in Simulation* 65, no. 3 (2004): 221-229. https://doi.org/10.1016/j.matcom.2003.12.001

[24] Kumar, Subodh. "Natural convective heat transfer in trapezoidal enclosure of box-type solar cooker." *Renewable Energy* 29, no. 2 (2004): 211-222. https://doi.org/10.1016/S0960-1481(03)00193-9
[25] Rosali, Haliza, Mohd Noor Badlilshah, Mohamat Aidil Mohamat Johari, and Norfifah Bachok. "Unsteady Boundary Layer Stagnation Point Flow and Heat Transfer over a Stretching Sheet in a Porous Medium with Slip Effects." *CFD Letters* 12, no. 10 (2020): 52-61. https://doi.org/10.37934/cfdl.12.10.5261
[26] Merrikh, A. A., and A. A. Mohamad. "Non-Darcy effects in buoyancy driven flows in an enclosure filled with vertically layered porous media." *International Journal of Heat and Mass Transfer* 45, no. 21 (2002): 4305-4313. https://doi.org/10.1016/S0017-9310(02)00135-7
[27] Phanikumar, M. S., and R. L. Mahajan. "Non-Darcy natural convection in high porosity metal foams." *International Journal of Heat and Mass Transfer* 45, no. 18 (2002): 3781-3793. https://doi.org/10.1016/S0017-9310(02)00089-3
[28] Baytas, A. C., A. F. Baytas, D. B. Ingham, and I. Pop. "Double diffusive natural convection in an enclosure filled with a step type porous layer: Non-Darcy flow." *International Journal of Thermal Sciences* 48, no. 4 (2009): 665-673. https://doi.org/10.1016/j.ijthermalsci.2008.06.001
[29] Sheremet, Mikhail Alexandrovich, and Ioan Pop. "Conjugate natural convection in a square porous cavity filled by a nanofluid using Buongiorno's mathematical model." *International Journal of Heat and Mass Transfer* 79 (2014): 137-145. https://doi.org/10.1016/j.ijheatmasstransfer.2014.07.092
[30] Murshed, S. M. S., K. C. Leong, and C. Yang. "Enhanced thermal conductivity of TiO2-water based nanofluids." *International Journal of Thermal Sciences* 44, no. 4 (2005): 367-373. https://doi.org/10.1016/j.ijthermalsci.2004.12.005
[31] Halim, Nur Fazlin Che, and Nor Azwadi Che Sidik. "Mixing Chamber for Preparation of Nanorefrigerant." *Journal of Advanced Research in Applied Sciences and Engineering Technology* 21, no. 1 (2020): 32-40. https://doi.org/10.37934/araset.21.1.3240
[32] Kladias, N., and V. Prasad. "Natural convection in horizontal porous layer: Effects of Darcy and Prandtl numbers." *Journal of Heat Transfer* 111 (1989): 926-935. https://doi.org/10.1115/1.3250807
[33] Varol, Yasin, Hakan F. Oztop, and Ioan Pop. "Numerical analysis of natural convection in an inclined trapezoidal enclosure filled with a porous medium." *International Journal of Thermal Sciences* 47, no. 10 (2008): 1316-1331. https://doi.org/10.1016/j.ijthermalsci.2007.10.018
[34] Varol, Yasin, Hakan F. Oztop, and Ahmet Koca. "Effects of inclination angle on natural convection in composite walled enclosures." *Heat Transfer Engineering* 32, no. 1 (2011): 57-68. https://doi.org/10.1080/01457631003732920
[35] Boussinesq, Joseph. "Théorie Analytique De La Chaleur Mise En Harmonie Avec La Thermodynamique Et Avec La Théorie Mécanique De La Lumière." *Monatshefte für Mathematik und Physik* 15, no. 1 (1904). https://doi.org/10.1007/BF01692408
[36] Khanafer, Khalil, Kambiz Vafai, and Marilyn Lightstone. "Buoyancy-driven heat transfer enhancement in a two-dimensional enclosure utilizing nanofluids." *International Journal of Heat and Mass Transfer* 46, no. 19 (2003): 3639-3653. https://doi.org/10.1016/S0017-9310(03)00156-X
[37] Lauriat, G., and V. Prasad. "Non-Darcian effects on natural convection in a vertical porous enclosure." International *Journal of Heat and Mass Transfer* 32, no. 11 (1989): 2135-2148. https://doi.org/10.1016/0017-9310(89)90120-8
[38] Ameur, Houari. "Effect of the baffle inclination on the flow and thermal fields in channel heat exchangers." *Results in Engineering* 3 (2019): 100021. https://doi.org/10.1016/j.rineng.2019.100021
[39] Ameur, Houari. "Effect of corrugated baffles on the flow and thermal fields in a channel heat exchanger." *Journal of Applied and Computational Mechanics* 6, no. 2 (2020): 209-218.
[40] Kaid, Noureddine, and Houari Ameur. "Enhancement of the performance of a static mixer by combining the converging/diverging tube shapes and the baffling techniques." *International Journal of Chemical Reactor Engineering* 18, no. 4 (2020). https://doi.org/10.1515/ijcre-2019-0190
[41] Menni, Younes, Ali J. Chamkha, Giulio Lorenzini, Noureddine Kaid, Houari Ameur, and Mohammed Bensafi. "Advances of nanofluids in solar collectors-a review of numerical studies advances of nanofluids in solar collectors-a review of numerical studies." *Mathematical Modelling of Engineering Problems* 6, no. 3 (2019): 415-427.

https://doi.org/10.18280/mmep.060313
[42] Mahammedi, Abdelkader, Houari Ameur, Younes Menni, and Driss Meddah Medjahed. "Numerical Study of Turbulent Flows and Convective Heat Transfer of Al2O3-Water Nanofluids In A Circular Tube." *Journal of Advanced Research in Fluid Mechanics and Thermal Sciences* 77, no. 2 (2020): 1-12. https://doi.org/10.37934/arfmts.77.2.112
[43] Menni, Younes, Ali J. Chamkha, and Houari Ameur. "Advances of Nanofluids in Heat Exchangers-A Review." *Heat Transfer* 49, no. 8 (2020): 4321-49. https://doi.org/10.1002/htj.21829